

A Novel Fuzzy Inference System Based Robust Reversible Watermarking Technique provided with Six Layer Security

V.Belmer Gladson¹, Dr.R.Balasubramanian²

Research Scholar¹, Professor²

Department of CSE, M.S University, Tirunelveli, Tamil Nadu, India

Abstract: Digital Watermarking has evolved as one of the latest technologies for digital media copyright protection. Watermarking of images can be done in many ways and one of the proposed algorithms for image watermarking is by utilizing Fuzzy Logic. It is similar to the concept of a Fuzzy set, each element can be defined by an ordered pair, in which one is the value and other is the membership function value. Fuzzy logic systems can explain inaccurate information and explain their decisions. Fuzzy inference system is the simplest way of performing Fuzzy Logic. In the proposed method, three Fuzzy inference models are used to generate the weighing factor for embedding the watermark and input to the Fuzzy Inference System is taken from the Human Visual System model. The Performance measures used in the Process are Peak Signal to Noise Ratio (PSNR), Structural Similarity Index (SSIM), Normalized Cross Correlation (NCC) and Bit Error Ratio (BER). The Proposed algorithm is immune to various Image Processing attacks.

Keywords: *Digital Image Watermarking; Discrete Wavelet Transform; Fuzzy Inference System; Normalized Cross Correlation; Peak Signal to Noise Ratio.*

1. INTRODUCTION

A digital watermark is a kind of marker covertly embedded in a noise-tolerant such as an audio, video or image data. It is typically used to identify ownership of the copyright of such images. Watermarking is the process of hiding digital information. Digital watermarks may be used to verify the authenticity or integrity to show the identity of its owners. It is prominently used for tracing copyright infringements and for banknote authentication [1]. Traditional Watermarks may be applied to visible media (like images or video), whereas in digital watermarking, the data may be audio, pictures, video, texts or 3D models. For marking media files with copyright information, a digital watermark has to be rather robust against modifications. Instead, if integrity has to be ensured, a fragile watermark would be applied.

Digital watermarking tries to control the robustness as top priority. Digital watermarking techniques have been indicated so far as a possible solution when, in a specific application scenario (Authentication, Copyright Protection, Finger printing, etc.), there is the need to embed an informative message in a digital document in an imperceptible way. Such a goal is basically achieved by performing a slight modification to the original data trying to, at the same time; satisfy other bindings such as capacity and robustness. The watermarked content is different from the original one. This means that any successive assertion, usage, and evaluation must happen on a, though weakly, corrupted version, if original data have not been stored and are not readily available. It is now clear that the dependence of the application scenario, this cannot always be accepted. The watermarking process is zero impact but, allows at the same time, to convey an informative message. Watermarking can be classified as either Visible Watermarking or Invisible Watermarking.

2. LITERATURE SURVEY

Shuang Yi, Yicong Zhou, and Zhongyun Hua [2] proposed an inverse method for hiding natural image data using block level prediction and error propagation. This method can embed confidential data into 2×2 blocks of images with extra pixels in each block. Extending this concept to encrypted domains, the authors propose an inverse method for hiding data in encrypted images using the Adaptive Level Prediction and Error Extraction (ABPEERDHEI). ABPEE-RDHEI encrypts the original image by rearranging the block to prevent data embedded asymmetry and applying a stream stream to the block that allowed the image to further enhance the security level. Thanks to the pixel-adaptor and embedded selection, ABPEE-RDHEI can

achieving high levels of embeddedness and quality of encrypted images. The results and the original analysis show that ABPEE-RDHEI performed better than the current method. Yan Qi and Liping Liu [3] proposed a reversible water recognition algorithm with low color illusion.

By analyzing the correlation of different color components in the color image and amplifying the pixels predicted by the adaptive forecasting operator, data, water marking and retrieval of the original image. Experiments have shown that a given algorithm performs better than other classical color image algorithms and can retrieve the original image without loss. Digital water marking can be carried out in the domain or frequency range. The amplitude regression technique changes the pixel values in the image overlap with different algorithms. In the Territory is Chan Sykel. L.M. [4] Alternatives of the proposed LBS can be used to integrate the partitioned information into the cover. With the LB1 technique, a bit of text is replaced by unremarkable pixel images. The LB technique is simple and has low computational complexity. A Hello-based LB method for hiding messages in images was proposed by Mark Hassan et al. In [5]. They used the LDS replacement technique to embed water markers and water markers based on the spiral replacement algorithm. J. Feng, I. Lin, C. Tsai, Y. Chu [6] over the years, there has been some research work on reverse water markers. Reverse water marking is an early type of water marking scheme. Not only can it increase the ownership of the original media, but it can also restore the original media entirely from the printer. This feature is suitable for a number of major media outlets such as medical and military imaging, as these types of media do not allow loss. The purpose of this document is to identify the purpose of reverse water markers that reflect current progress and to provide some scientific issues for the future. Liu and Jay Ying [7] proposed a colorblind, color-blind adaptive image resolution algorithm. The proposed algorithm increases the ability to attack the hidden features of the image, improves the detection security, and has greater resistance to noise, cut, and attack of JPEG compression. Khumb Biphavar, Bavana Palai and Drs. Sardana K. Mishra [8] proposed a method of water marking. This method uses conditioned local forecasts and produces better results. The general idea of digital water marking is to incorporate data

into the media to ensure data security. The water filtration technique that meets these requirements is known as reverse water filtration.

Many reversible visible watermarking schemes are proposed in the past [9–14]. Hu and Jeon [9] proposed a scheme by modifying one significant bit plane of the pixels to achieve watermark visibility. Then, they compressed the altered bit plane values as recovery information which was embedded into the non-watermarked image region for lossless recovery. However, the watermarked image often distorts rather significantly compared with the original image. In [10], the reversible watermarking scheme based on deterministic one-to-one compound mappings of image pixel values has been proposed. Chen et al. [11] proposed a scheme based on the conventional difference expansion technique. In this scheme, the cover image is divided into nonoverlapping blocks and each block is embedded with one watermark bit. But unfortunately, there is a large amount of overflowing or underflowing pixels in the watermarked image. Once exceeded, the watermarked image cannot be recovered perfectly. In the scheme of [12] by Mohammad et al., the pixel circular shift operation is utilized to embed the watermark into the block truncation coding-compressed (BTC-compressed) image. According to the parity of the bit plane, the watermark signal can be extracted reversibly. In the abovementioned reversible visible watermarking schemes, the watermark embedding region is specified, which is generally the center of the cover image. In [13], Qi et al. proposed a reversible visible scheme based on the human visual system (HVS) and region of interest (ROI) selection. For watermark embedding, HVS is adopted to modify the pixel values so as to get a better effect of watermark visibility. And, the ROI selection strategy is designed to find the flat regions with low or high luminance for watermark embedding. The chosen flat regions usually do not contain abundant information which can be easily cropped but without affecting the whole information of images. However, to maintain the copyright of the images better, the visible watermark should be embedded into the subject region of the image which contains the most important image information.

Hence, the selected ROI for watermark embedding in [13] may be not suitable. To select the subject region of images, we proposed a novel ROI selection strategy based on Grad-CAM [15] for visible watermark embedding. With this novel ROI selection strategy, the visible watermark can be embedded in the subject region to protect the copyright of images. However, the visible watermark into the subject region can degrade the watermarked image quality. The key to solving this problem is to balance the watermark visibility and the watermarked image quality, which means the embedded watermark should not be so significant that the watermarked image details have been covered too much [17, 18]. Motivated by the scheme proposed by Yao et al. [14], the enhanced JND model [16] has been utilized in this paper to obtain the tradeoff between watermark visibility and watermarked image quality.

Generally, a reversible visible watermarking technique is used to protect and maintain the copyright. The region of visible watermark embedding is vital. Assuming that the watermark embedding region is not the subject of an image, it can be easily modified or cropped for malicious use. However, there is no scheme proposed in the past to select the main body region as ROI for visible watermark embedding.

The fuzzy theory has been widely used in image compression [19], image reconstruction [20], image segmentation [21] and image object detection [22], etc. The combination of fuzzy theory and digital watermarking is due to the uncertainty of image characteristic definition. The FIS has a good control effect on this time-varying, nonlinear system that cannot establish an accurate mathematical model [23].

Several adaptive watermarking methods have been proposed in the past, the main purpose of which was to use fuzzy knowledge to achieve a balance between robustness and imperceptibility [24, 25]. An image watermarking algorithm based on dynamic fuzzy inference system (DFIS) was proposed in [26]. The algorithm used the human visual system (HVS) model to extract the sensitivity knowledge of human eyes. In [27], Mortezaei and Mohammad developed a new watermarking method based on fuzzy integration

to obtain the similarity between the discrete cosine transform (DCT) coefficients of the original image and the watermark signal. Jagadeesh et al. [28] proposed a blind image watermarking using neural network and fuzzy logic, which were combined to form a hybrid intelligence technology of neural fuzzy system. In the embedding and extraction stages, the output of FIS-BPNN was taken as the weight factor. Compared with other methods, this algorithm made the watermark invisible and robustness against filtering, rotation, compression, image blur and other watermark attacks.

3. METHODOLOGY

This work uses the wavelet transform (DWT), the Arnold transform (ET), the Chaos-Based Encoding (CBE), the reasoning prediction using the robotic model, and the sorting of prediction error algorithms. The following subsections give a brief explanation of each algorithm. This section describes the general base concepts used in the proposed water marking scheme.

- DWT transform is used to insert the watermark in imperceptible manner. The watermark bits are inserted in the significant coefficients sub-bands by considering the human visual system (HVS) characteristics.
- CBE technique is used to encode the character text before embedding it in the image.
- Arnold Transform is used to make the watermark more secure and protect the embedded data.
- Prediction and prediction error sorting algorithm are used to find the best position to embed the watermark data increase the quality of watermarking

Fuzzy inference System

The principle of fuzzy logic reaches the human approach in the sense that the variables treated are not binary but of variable linguistic relatives of human language as high contrast, a lot more clearly, very textured, very homogeneous etc. Moreover, these linguistic variables are processed with rules that refer to some knowledge of system. The fuzzifier and the defuzzifier have the role of converting external information in fuzzy quantities and vice versa. FIS as in Fig.1 consists of four function blocks. They are

1. **Fuzzifier:** It transfers the crisp input to fuzzy sets.
2. **Knowledge Base:** It mainly consists of

atabase and rule base. The data base defines the membership functions of the linguistic variables. The rule base consists of a set of IFTHEN rules that can be given by a human expert or also can be extracted from the linguistic description of the data.

d

3. **Inference Engine:** It is a general control mechanism that exploits the fuzzy rules and the fuzzy sets defined in the Knowledge Base in order to reach certain conclusion.
4. **De-Fuzzifier:** It transfers the fuzzy sets into crisp outputs.

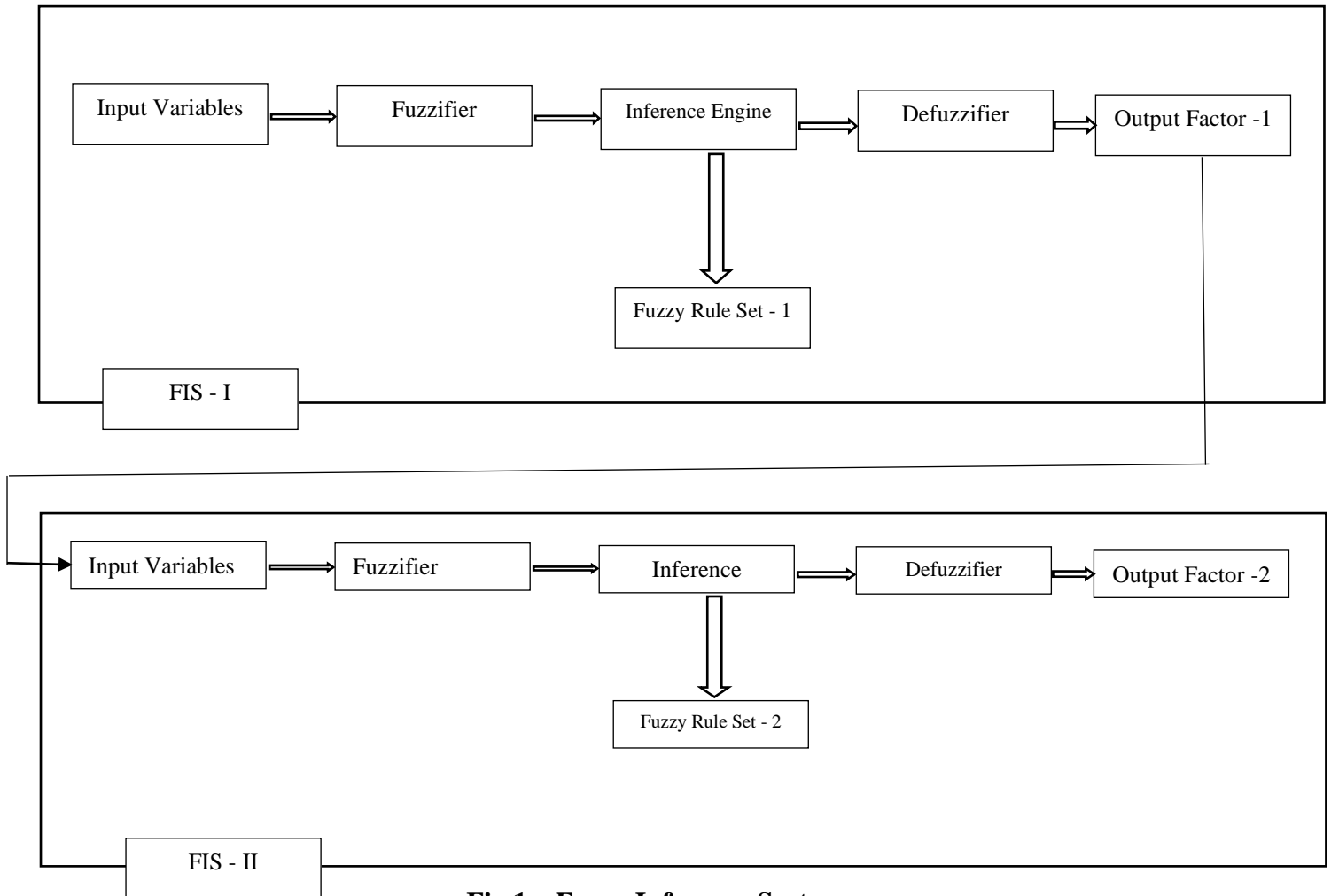


Fig 1 – Fuzzy Inference System

3.1 PROPOSED SYSTEM

The materials, input image datasets, and methods used to the overall system of our proposed approach is illustrated in Fig 2 & Fig 3. Our proposed system consist of two phases such as watermark embedding phase and watermark extraction phase. In embedding phase, first the input image is pre-processed by using Arnold transform and then DWT is applied onto the pre-processed image. And then the DWT transformed image is divided into 4 sub blocks. After dividing the sub blocks, the next step is to

shuffle the sub blocks to differentiate between the homogenous and non-homogenous blocks. After shuffling the next step is to apply the prediction and find the prediction error. Then the prediction error value is sorted to generate the places for embedding the watermark bit. At this stage, the watermark image is get from the user and these images are also Pre-

Processed and encrypted. These encrypted watermark image pixels are embedded with the sorted prediction error values. Finally, the homogenous and non-homogenous

blocks are combined and the four sub blocks are also combined to generate the single image. After that inverse DWT and Arnold transform is applied to produce the watermarked image.

In extraction phase, first the watermarked image is pre-processed by using Arnold transform and then DWT is applied onto the pre-processed image. And then the DWT transformed image is divided into 4 sub blocks. After dividing the sub blocks, the next step is to shuffle the sub blocks to differentiate between the homogenous and non-homogenous blocks. After shuffling the next step is

to apply the prediction and find the prediction error. Then the prediction error value is sorted to get the places for extracting the watermark bit. At this stage, the watermark bit are extracted and then it is decrypted. These decrypted watermark image is considered as the output watermark image. Finally, the homogenous and non-homogenous blocks are combined and the four sub blocks are also combined to generate the single image. After that inverse DWT and Arnold transform is applied to produce the original image.

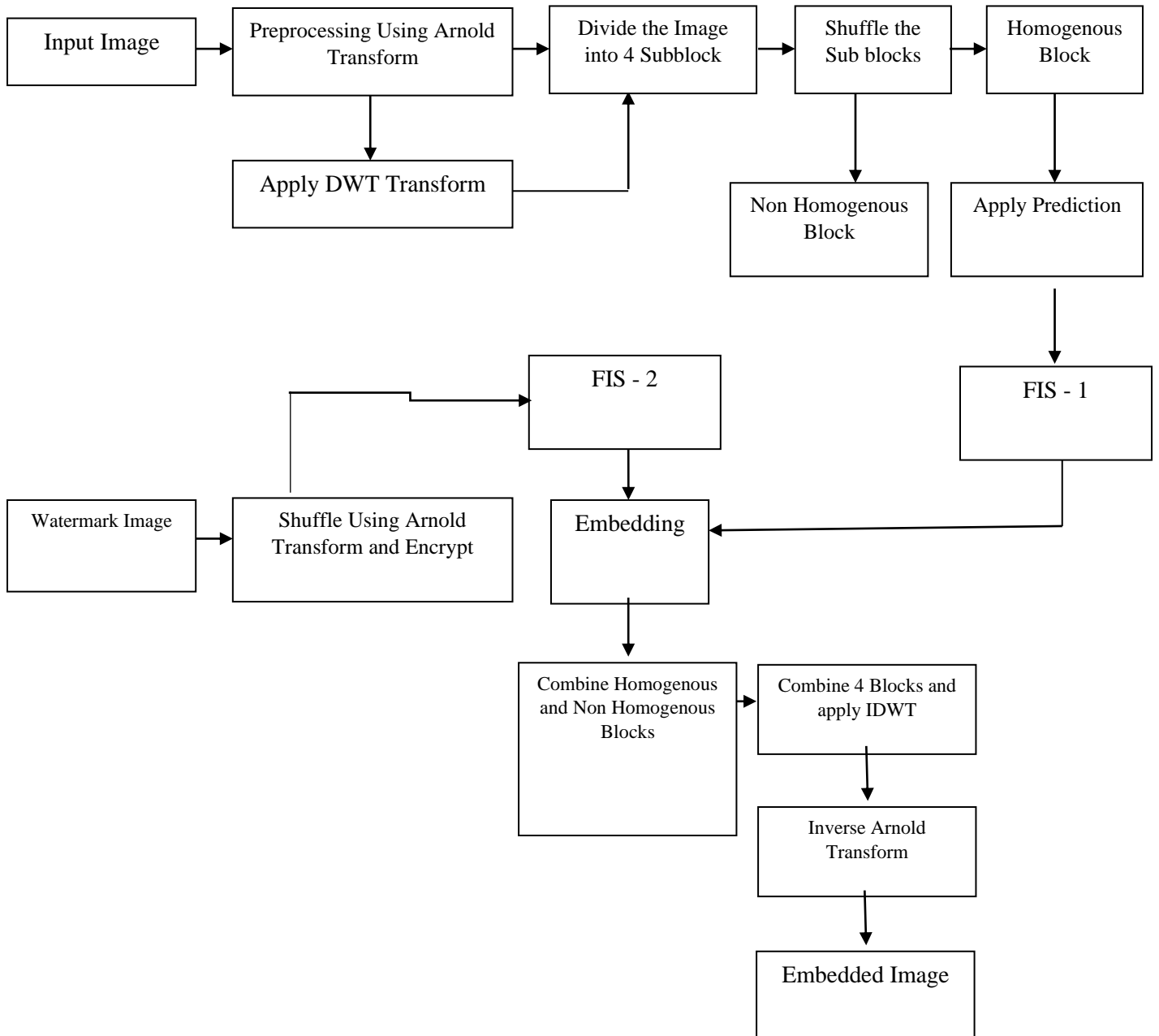


Fig 2 - Block diagram of embedding algorithm

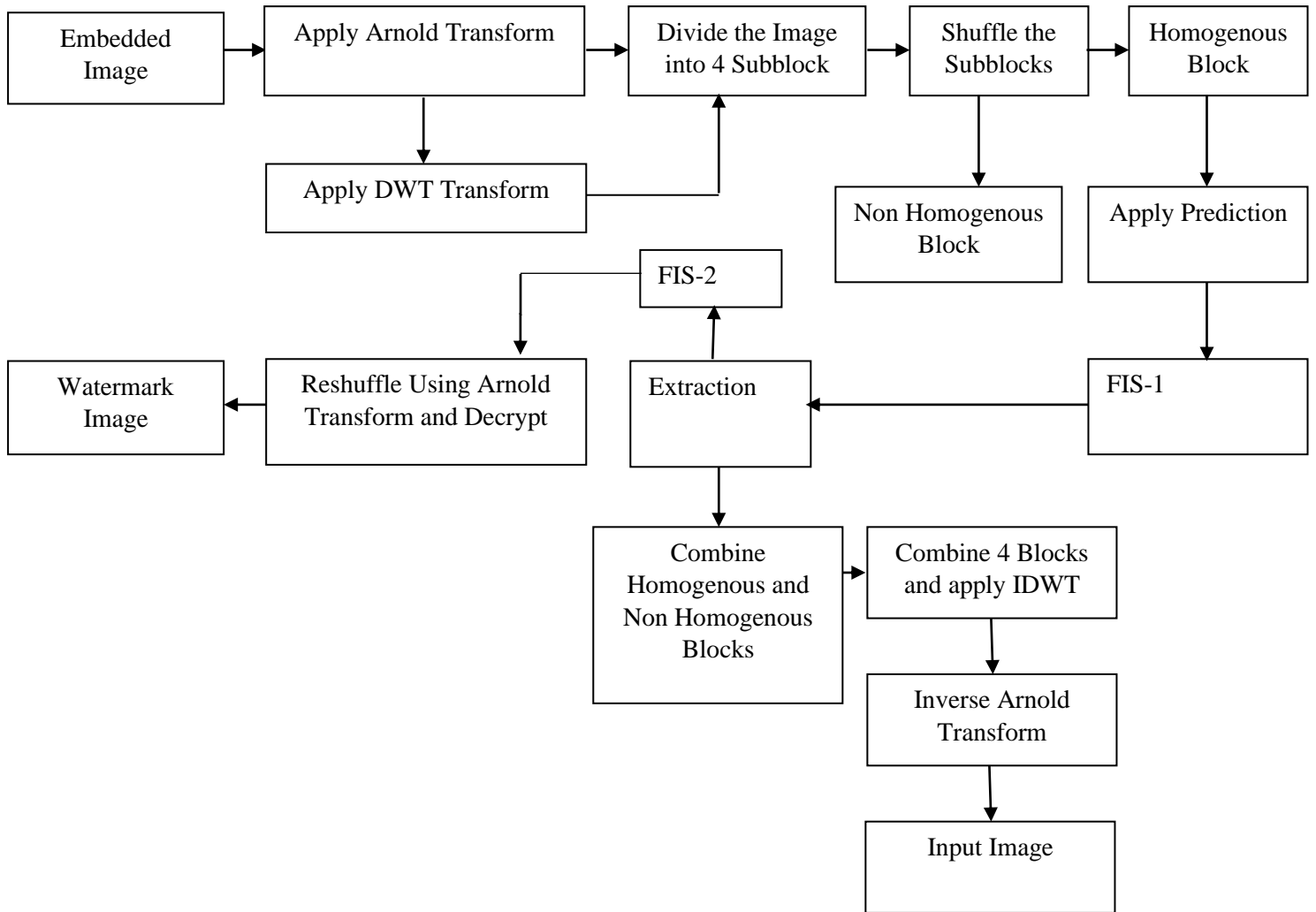


Fig 3 - Block diagram of extracting algorithm

The proposed method integrates the human visual characteristics of the document image watermark embedded sub-block, with a multidimensional fuzzy inference perceptual model. In this paper, an adaptive visible document image watermarking method is proposed with the contribution of using the two-stage fuzzy inference system. First, because the visible watermark embedded in the blank edge of the document image will be easily cut out, the algorithm fixes the watermark embedding position in the center of the document image. The visible watermark is spatially inseparable from the center content of the document image. Second, because the visible watermark embedding process will inevitably change the overall brightness, the white pixels of the binary watermark

are filtered out. The watermark embedding formula is simplified to:

$$I_{i,j}^W = \begin{cases} I_{i,j} \times factor_{x,y}, & \text{if } W_{x,y} = 0, \\ I_{i,j}, & \text{if } W_{x,y} = 1. \end{cases} \dots\dots\dots(1)$$

Where $W_{x,y}$ and $factor_{x,y}$ are the (x, y) th pixels of the binary watermark signal and the embedding intensity factor, respectively.

The intensity factor is expressed in a range of [0, 1]. The value '0' represents that the gray value of this pixel is 0; that is, the watermark at the embedded position is opaque. Analogously, a value of '1' indicates that the gray value of this pixel does not change; in other words, the watermark at the embedded

Sort Prediction Error

position is transparent to the human perception system. When factor is between 0 and 1, the embedding strength of the black pixel of the watermark is controlled. The proposed watermarking scheme is a permanent visible watermark, so the watermark extraction process is not needed. General watermarking attack algorithms, such as adding noise, image compression, filtering and geometric transformation, will cause degradation of the host document image itself. Therefore, visibility watermarking algorithms mainly consider watermark removal attacks. As shown in Fig.2 & Fig.3, in order to avoid the Reversible watermark being removed, the peak value of the probability histogram of the embedded watermark document image is searched. The way to eliminate this peak is to distribute it evenly across all the gray levels of the document image. The selected uniform distribution function is defined as follows:

$$f(\text{random-gray}) = \begin{cases} \frac{1}{b-a}, & \text{if random-gray} \in [a, b], \\ 0, & \text{others.} \end{cases} \dots\dots\dots(2)$$

A. Embedding Algorithm:

The procedure for embedding the watermark is:

1. Original Image is 512 X 512 pixels gray scale image and Original Watermark is 64x64 pixels binary image as input.
2. Divide the cover image (gray scale) into 8x8 blocks and apply DWT to each block.
3. Calculate LL, HL, LH and HH for each block.
4. Provide cover image prediction result as input to FIS-1, Watermarked Encrypt image as input to FIS-2.
5. The outputs of FIS-1 and FIS-2 are given as inputs, the output obtained is used as weighing factor.
6. Centre value in each block is taken as embedding location, and embedding is done utilizing the embedding formula,
if $w=1$
 $X' = (s1(i) * s2(i));$
else

$$X' = (s1(i) + s2(i));$$

end

where X' = new DWT component,

$s1, s2$ are FIS-1, FIS-2 outputs.

7. Take DWT for every block and recombine the blocks to form the watermarked image.
8. Calculate PSNR for the watermarked and original image.

B. Extraction Algorithm:

The watermark mining method is as per trails:

1. The Image is 512 X 512 gray scale image as input.
2. Divide the watermarked image (gray scale) into 8x8 blocks and apply DWT to each block.
3. Calculate LL, HL, LH and HH for each block.
4. Provide embedded image prediction result as input to FIS-1, Extracted Watermarked image as input to FIS-2.
5. Centre value in each block is taken and extraction is done utilizing the inverse of embedding formula,
if $X'' - (s1(i) * s2(i)) > 0$
 $w=1$
else
 $w=0$
end
where X'' = DWT component of watermarked image,
 $s1, s2$ are FIS-1, FIS-2 outputs.
6. Rearrange the watermark bits to form 64x64 watermark image.
7. Calculate NCC for the extracted and original watermark.

3.2 PERFORMANCE ANALYSIS

A. Experimental Images

Experiments were conducted on a group of standard ieee images to verify the effectiveness of the proposed scheme. All of these images are 512 × 512 images. These images are used as cover image. For watermarking purpose 256 × 256 size logo images are used. Some of the images are shown in Fig 4.

B. Performance Analysis

To evaluate the performance of the proposed method, performance metrics such as Peak Signal-to-Noise Ratio (PSNR), Structural Similarity Index (SSIM), Normalized Cross-Correlation (NCC) and Bit Error Ratio (BER) are used:

B1.

Peak Signal-to-Noise-Ratio (PSNR):

The peak signal-to-noise ratio (PSNR) is used to evaluate the quality between the attacked image and the original image. The PSNR formula is defined as follows: (Where MAX = 255)

$$PSNR = 10 \log_{10} \left(\frac{MAX^2}{MSE} \right) \dots\dots\dots(3)$$

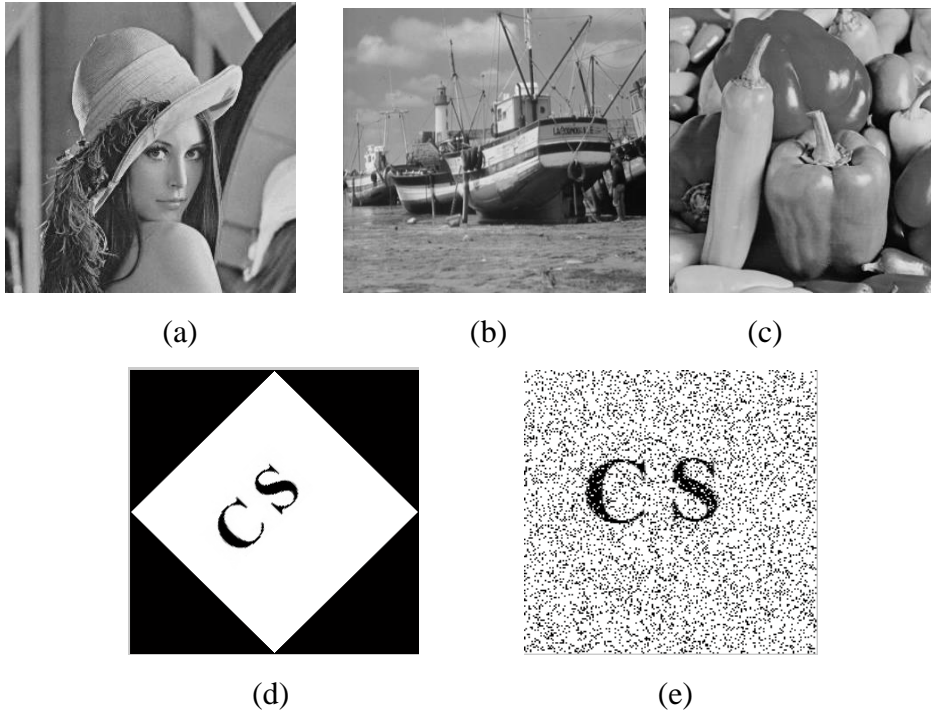


Fig 4 - Expiremental Images

B2. Structural Similarity Index

The SSIM Index quality assessment index is based on the computation of three terms, namely the luminance term, the contrast term and the structural term.

$$SSIM = \frac{(2\mu_x\mu_y + C_1)(2\sigma_{xy} + C_2)}{(\mu_x^2 + \mu_y^2 + C_1)(\sigma_x^2 + \sigma_y^2 + C_2)} \dots\dots\dots(4)$$

Where $\mu_x, \mu_y, \sigma_x, \sigma_y,$ and σ_{xy} are the local means, standard deviations, and cross-covariance for images x, y . If $\alpha = \beta = \gamma = 1$ (the default for Exponents), and $C_3 = C_2/2$ (default selection of C_3)

B3. Normalised Cross-Correlation (NCC)

This is one of the important parameter for calculating the robustness. The robustness is evaluated by using Normalized Cross-Correlation (NC) is shown below:

$$NCC(k, \bar{k}) = \frac{\sum_{i=1}^M \sum_{j=1}^N [k(i,j) - \mu_k][\bar{k}(i,j) - \mu_{\bar{k}}]}{\sqrt{\sum_{i=1}^M \sum_{j=1}^N [k(i,j) - \mu_k]^2} \sqrt{\sum_{i=1}^M \sum_{j=1}^N [\bar{k}(i,j) - \mu_{\bar{k}}]^2}} \dots\dots\dots(5)$$

Where N and M represent the number of pixels in the watermark, k, \bar{k} indicates to the original watermark and the extracted watermark, the correlation coefficient can be between -1 and 1. If the NC value is near +1, then the extracted watermark is strongly correlated.

B4. Bit Error Ratio (BER)

This

is one of the parameter used for calculating the error value of the retrieved watermark image. The BER can be calculated as follows:

$$BER = \frac{1}{P} \sum_{i=1}^N |w_{out}(i) - w_{in}(i)| \dots\dots\dots(6)$$

Where w_{out} is the extracted watermark, w_{in} is the original watermark and P is the size of the watermark

4. RESULTS AND DISCUSSION

In order to explore the performance of the proposed watermarking algorithm, MATLAB platform is used and a number of experiments are performed on different images. To test the robustness of the algorithm PSNR values are evaluated between original images and modified images. Except noise attack all the remaining attacks are resistant to the attacks. The embedding strength is based on the HVS properties of the images.

4.1 Type of Attacks

To examine the issue of robustness of the proposed embedding scheme, the watermarked images are subject to eight different image processing attacks. These are

Salt & Pepper Noise

Salt-and-pepper noise is a form of noise sometimes seen on images. It is also known as impulse noise. This noise can be caused by sharp and sudden disturbances in the image signal. It presents itself as sparsely occurring white and black pixels.

Speckle Noise

Speckle noise is an undesirable effect. The source of this type of noise is caused due to random interference between the coherent returns issued from the so many scatterers present on a earth surface, on the scale of a wavelength of the incident radar wave.

Gaussian Noise

Gaussian noise, named after Carl Friedrich Gauss, is statistical noise having a probability density function (PDF) equal to that of the normal distribution, which is also known as the Gaussian distribution. In other words, the values that the noise can take on are Gaussian-distributed.

Rotation

Image rotation is a common image processing routine with applications in matching, alignment, and other image-based algorithms. The input to an image rotation routine is an image, the rotation angle θ , and a point about which rotation is done.

Histogram Equalization

Histogram equalization is a method to process images in order to adjust the contrast of an image by modifying the intensity distribution of the histogram. The objective of this technique is to give a linear trend to the cumulative probability function associated to the image.

JPEG Compression

JPEG stands for Joint photographic experts group. It is the first international standard in image compression. It is widely used today. It could be lossy as well as lossless. But the technique we are going to discuss here today is lossy compression technique.

Median Filtering

The median filter is a non-linear digital filtering technique, often used to remove noise from an image or signal. Such noise reduction is a typical pre-processing step to improve the results of later processing

Weiner Filter

the Wiener filter is a filter used to produce an estimate of a desired or target random process by linear time-invariant (LTI) filtering of an observed noisy process, assuming known stationary signal and noise spectra, and additive noise. The Wiener filter minimizes the mean square error between the estimated random process and the desired process.

Gaussian Filtering

A Gaussian filter is a linear filter. It's usually used to blur the image or to reduce noise. The Gaussian filter alone will blur edges and reduce contrast. The Median filter is a non-linear filter that is most commonly used as a simple way to reduce noise

in
an image.

Scaling

Image scaling is the process of resizing a digital image. Scaling down an image makes it smaller while scaling up an image makes it larger.

Crop

Cropping is the removal of unwanted outer areas from a photographic or illustrated image. The process usually consists of the removal of some of the peripheral areas of an image to remove extraneous trash from the picture, to improve its framing, to change the aspect ratio, or to accentuate or isolate the subject matter from its background.

Table 1 – PSNR of the Extracted Watermark under Different Attacks

ATTACKS	DCT BASED FUZZY –BPN			RW – FLS			Proposed RW - SLS		
	LENA	PEPPER	BOAR	LENA	PEPPER	BOAT	LENA	PEPPER	BOAT
Salt & Pepper Noise (D=0.3)	28.45	30.85	31.16	40.15	44.23	45.56	41.03	45.20	46.16
Salt & Pepper Noise (D=0.01)	28.36	31.26	32.29	41.46	44.56	45.55	42.46	45.26	46.55
Salt & Pepper Noise (D=0.001)	28.59	32.48	33.45	40.56	44.89	45.81	41.36	45.89	46.81
Salt & Pepper Noise (D=0.005)	29.14	32.95	33.49	40.84	45.23	46.18	41.64	46.23	47.32
Speckle Noise (var=0.01)	29.58	32.18	33.57	40.26	43.12	44.51	41.10	44.10	45.98
Speckle Noise (var=0.04)	28.67	31.28	32.69	40.16	44.89	45.52	41.02	45.19	46.52
Speckle Noise (var=0.4)	28.45	30.85	32.85	40.45	44.78	45.21	41.22	45.18	46.03
Gaussian Noise (M=0, var=0.01)	29.38	30.57	31.85	40.21	44.72	45.58	41.01	45.12	46.00
Gaussian Noise (M=0, var=0.05)	29.84	31.75	32.86	40.19	43.52	44.89	41.09	44.40	45.01
Gaussian Noise (M=0, var=0.5)	28.39	31.27	32.06	40.24	43.89	44.54	41.14	44.79	46.05
Rotation (angle 45°)	29.86	30.86	31.23	40.16	44.28	44.87	41.03	45.28	46.01
Rotation (angle 110°)	28.16	30.29	31.26	41.21	44.27	45.54	42.10	45.20	46.40
Rotation (angle -50°)	29.46	32.64	33.27	40.56	43.56	44.62	41.23	44.42	45.26
Histogram Equalization	29.92	31.62	32.27	40.56	42.56	43.45	41.52	43.44	44.04
JPEG Compression (Q=20)	28.1	31.68	32.54	41.57	42.15	43.01	42.02	43.02	44.94
JPEG Compression (Q=40)	28.15	30.45	31.28	40.16	44.67	45.26	41.67	45.06	46.10

JPEG Compression (Q=60)	28.35	31.92	32.84	40.28	44.75	45.74	41.05	45.15	46.04
JPEG Compression (Q=80)	29.51	32.84	33.62	40.76	44.52	45.24	41.06	45.03	46.01
JPEG Compression (Q=100)	28.92	30.16	30.51	41.64	43.82	44.66	42.46	44.08	45.06
Median Filtering (3 X 3)	28.16	31.28	31.68	40.57	44.28	45.52	41.28	45.90	46.02
Median Filtering (5 X 5)	29.38	32.94	33.92	40.64	43.67	44.92	41.10	44.10	45.09
Weiner Filtering (3X3)	29.84	31.28	32.08	40.27	44.27	45.69	41.20	45.27	46.60
Weiner Filtering (5X5)	28.96	32.61	33.17	41.68	44.19	45.44	42.09	45.19	46.04
Gaussian Filtering (3X3)	29.82	30.69	31.48	41.56	43.17	44.88	42.56	44.98	45.08
Gaussian Filtering (5X5)	28.74	30.49	30.61	40.28	43.89	44.99	41.18	44.02	45.09
Scaling (zoomout=0.5, zoomin=2)	29.68	31.23	32.64	40.96	44.68	45.24	41.17	45.24	46.24
Scaling (zoomout=0.25, zoomin=4)	29.38	32.82	33.85	40.82	42.95	43.58	41.08	43.90	44.58
Scaling (zoomout=2, zoomin=6)	28.49	31.27	32.82	41.24	43.61	44.41	42.24	44.06	45.06
Crop 10	28.81	31.06	31.84	41.26	44.38	45.51	42.05	45.26	46.38
Crop 20	28.64	32.08	32.94	41.85	42.61	43.86	42.03	43.06	44.16
Crop 30	29.38	32.82	32.95	41.24	44.5	45.89	42.04	45.50	46.80

Table 2 – SSIM of the Extracted Watermark under Different Attacks

A TTACKS	DCT BASED FUZZY –BPN			RW – FLS			Proposed RW - SLS		
	LENA	PEPPER	BOAT	LENA	PEPPER	BOAT	LENA	PEPPER	BOAT
Salt & Pepper Noise (D=0.3)	27.45	29.85	31.16	39.15	43.23	44.56	44.03	45.20	46.16
Salt & Pepper Noise (D=0.01)	28.36	31.26	32.29	41.46	44.56	45.55	42.46	45.26	46.55
Salt & Pepper Noise (D=0.001)	28.59	32.48	33.45	40.56	44.89	45.81	41.36	45.89	47.81
Salt & Pepper Noise (D=0.005)	29.14	32.95	33.49	40.84	45.23	46.18	41.64	46.23	47.32
Speckle Noise (var=0.01)	29.58	32.18	33.57	40.26	43.12	44.51	41.10	44.10	45.98

Speckle Noise (var=0.04)	28.67	31.28	32.69	40.16	44.89	45.52	41.02	45.19	46.52
Speckle Noise (var=0.4)	28.45	30.85	31.85	40.45	44.78	45.21	41.22	45.18	46.03
Gaussian Noise (M=0, var=0.01)	29.38	30.57	30.85	40.21	44.72	45.58	41.01	45.12	46.00
Gaussian Noise (M=0, var=0.05)	29.84	31.75	32.86	40.19	43.52	42.89	41.09	44.40	45.01
Gaussian Noise (M=0, var=0.5)	28.39	31.27	32.06	40.24	43.89	44.54	41.14	44.79	46.05
Rotation (angle 45°)	29.86	30.86	31.23	40.16	44.28	45.87	41.03	45.28	46.01
Rotation (angle 110°)	28.16	30.29	31.26	41.21	44.27	45.54	42.10	45.20	46.40
Rotation (angle -50°)	29.46	32.64	33.27	40.56	43.56	44.62	41.23	44.42	45.26
Histogram Equalization	29.92	31.62	32.27	40.56	42.56	43.45	41.52	43.44	44.04
JPEG Compression (Q=20)	28.1	31.68	32.54	41.57	42.15	43.01	42.02	43.02	44.94
JPEG Compression (Q=40)	28.15	30.45	31.28	40.16	44.67	45.26	41.67	45.06	46.10
JPEG Compression (Q=60)	28.35	31.92	32.84	40.28	44.75	43.74	41.05	45.15	46.04
JPEG Compression (Q=80)	29.51	32.84	33.62	40.76	44.52	45.24	41.06	45.03	46.01
JPEG Compression (Q=100)	28.92	30.16	30.51	41.64	43.82	44.66	42.46	44.08	45.06
Median Filtering (3 X 3)	28.16	31.28	32.68	40.57	44.28	45.52	41.28	45.90	46.02
Median Filtering (5 X 5)	29.38	32.94	33.92	40.64	43.67	44.92	41.10	44.10	45.09
Weiner Filtering (3X3)	29.84	31.28	32.08	40.27	44.27	45.69	41.20	45.27	46.60
Weiner Filtering (5X5)	28.96	32.61	33.17	41.68	44.19	45.44	42.09	45.19	46.04
Gaussian Filtering (3X3)	29.82	30.69	31.48	41.56	43.17	44.88	42.56	44.98	45.08
Gaussian Filtering (5X5)	28.74	30.49	30.61	40.28	43.89	44.99	41.18	44.02	45.09
Scaling (zoomout=0.5, zoomin=2)	29.68	31.23	32.64	40.96	44.68	45.24	41.17	45.24	46.24
Scaling (zoomout=0.25, zoomin=4)	29.38	32.82	32.85	40.82	42.95	43.58	41.08	43.90	44.58
Scaling (zoomout=2, zoomin=6)	28.49	31.27	32.82	41.24	43.61	44.41	42.24	44.06	45.06
Crop 10	28.81	31.06	31.84	41.26	44.38	45.51	42.05	45.26	46.38

Crop 20	28.64	32.08	32.94	41.85	42.61	43.86	42.03	43.06	44.16
Crop 30	29.38	32.82	32.95	41.24	44.5	45.89	42.04	45.50	46.80

Table 3 – NCC of the Extracted Watermark under Different Attacks

A TTACKS	DCT BASED FUZZY –BPN			RW - FLS			Proposed RW - SLS		
	LENA	PEPPER	BOAT	LENA	PEPPER	BOAT	LENA	PEPPER	BOAT
Salt & Pepper Noise (D=0.3)	0.8546	0.8689	0.8741	0.9389	0.9458	0.9568	0.9589	0.9822	0.9865
Salt & Pepper Noise (D=0.01)	0.6856	0.7456	0.8947	0.9456	0.9368	0.9618	0.9589	0.9908	0.9908
Salt & Pepper Noise (D=0.001)	0.6845	0.7475	0.8994	0.9475	0.9528	0.9618	0.9578	0.9869	0.9869
Salt & Pepper Noise (D=0.005)	0.7856	0.7589	0.8974	0.9489	0.9634	0.9634	0.9549	0.9865	0.9865
Speckle Noise (var=0.01)	0.8879	0.9124	0.8952	0.9124	0.9657	0.9477	0.9546	0.9833	0.9933
Speckle Noise (var=0.04)	0.9712	0.9025	0.8873	0.9025	0.9204	0.9104	0.9521	0.9823	0.9753
Speckle Noise (var=0.4)	0.6623	0.7546	0.8704	0.9546	0.9908	0.9908	0.9513	0.9772	0.982
Gaussian Noise (M=0, var=0.01)	0.6856	0.7578	0.8979	0.9578	0.9666	0.9666	0.9489	0.9751	0.978
Gaussian Noise (M=0, var=0.05)	0.6853	0.7345	0.8925	0.9345	0.9617	0.9617	0.9478	0.9746	0.9772
Gaussian Noise (M=0, var=0.5)	0.7521	0.7689	0.8636	0.9589	0.9869	0.9869	0.9475	0.9686	0.9751
Rotation (angle 45°)	0.7894	0.8478	0.8983	0.9478	0.9823	0.9823	0.9458	0.9666	0.9746
Rotation (angle 110°)	0.6812	0.7389	0.8981	0.9389	0.9686	0.9686	0.9458	0.9657	0.9686
Rotation (angle -50°)	0.7854	0.8245	0.8984	0.9245	0.9751	0.9751	0.9456	0.9652	0.9666
Histogram Equalization	0.7894	0.8521	0.899	0.9521	0.9865	0.9865	0.9436	0.9649	0.9652
JPEG Compression (Q=20)	0.6843	0.7459	0.8983	0.8459	0.9201	0.912	0.9389	0.9634	0.9649
JPEG Compression (Q=40)	0.8854	0.9105	0.8988	0.9105	0.9411	0.9411	0.9389	0.9617	0.9634
JPEG Compression (Q=60)	0.6894	0.7254	0.8992	0.9254	0.9564	0.9564	0.9345	0.9588	0.9618
JPEG Compression (Q=80)	0.8856	0.9236	0.8995	0.9436	0.9746	0.9746	0.9274	0.9581	0.9618

JPEG Compression (Q=100)	0.87895	0.9189	0.8998	0.9589	0.9922	0.9922	0.9256	0.9578	0.9617
Median Filtering (3 X 3)	0.7835	0.8241	0.8982	0.9241	0.9581	0.9581	0.9254	0.9564	0.9588
Median Filtering (5 X 5)	0.7857	0.8456	0.895	0.8456	0.9421	0.9421	0.9249	0.9528	0.9581
Weiner Filtering (3X3)	0.7865	0.8274	0.8984	0.9274	0.9509	0.9509	0.9245	0.9509	0.9568
Weiner Filtering (5X5)	0.7898	0.8138	0.8974	0.9138	0.9404	0.9404	0.9245	0.9458	0.9564
Gaussian Filtering (3X3)	0.7875	0.8256	0.8987	0.9256	0.9652	0.9652	0.9241	0.9421	0.9509
Gaussian Filtering (5X5)	0.8854	0.9245	0.8987	0.9245	0.9649	0.9649	0.9138	0.9411	0.9477
Scaling (zoomout=0.5, zoomin=2)	0.8856	0.8012	0.8948	0.8012	0.9356	0.9356	0.9124	0.9404	0.9421
Scaling (zoomout=0.25, zoomin=4)	0.7876	0.8249	0.8788	0.9249	0.9588	0.9588	0.9105	0.9382	0.9411
Scaling (zoomout=2, zoomin=6)	0.7845	0.8458	0.8992	0.9458	0.9772	0.9772	0.9025	0.9368	0.9404
Crop 10	0.7876	0.8549	0.8994	0.9549	0.9833	0.9833	0.9623	0.9356	0.9653
Crop 20	0.7872	0.8513	0.8989	0.9513	0.9382	0.982	0.9526	0.9204	0.9758
Crop 30	0.7873	0.8458	0.8986	0.9458	0.9578	0.978	0.9563	0.9201	0.9892

Table 4 – BER of the Extracted Watermark under Different Attacks

ATTACKS	DCT BASED FUZZY –BPN			RW - FLS			Proposed RW - SLS		
	LENA	PEPPER	BOAT	LENA	PEPPER	BOAT	LENA	PEPPER	BOAT
Salt & Pepper Noise (D=0.3)	12.46	11.49	10.34	8.56	7.24	6.29	5.23	6.01	5.66
Salt & Pepper Noise (D=0.01)	12.49	11.34	10.34	8.49	7.59	7.15	4.33	4.58	4.44
Salt & Pepper Noise (D=0.001)	11.67	10.49	10.34	7.48	6.49	6.34	4.39	4.96	4.56
Salt & Pepper Noise (D=0.005)	11.62	10.49	11.37	7.35	6.57	6.34	4.98	6.13	5.23
Speckle Noise (var=0.01)	12.76	11.57	10.46	8.15	7.29	7.48	5.26	6.58	5.99
Speckle Noise (var=0.04)	12.96	11.49	10.46	8.69	7.34	6.45	5.63	5.98	5.74
Speckle Noise (var=0.4)	11.06	10.59	12.48	7.2	6.89	6.57	4.56	4.65	4.6

Gaussian Noise (M=0, var=0.01)	11.45	10.64	10.49	7.56	6.24	6.58	6.18	6.98	6.24
Gaussian Noise (M=0, var=0.05)	12.49	11.57	10.49	8.24	7.49	6.68	5.82	5.69	5.72
Gaussian Noise (M=0, var=0.5)	11.67	10.64	10.49	7.34	6.35	7.16	5.75	5.98	5.82
Rotation (angle 45°)	12.57	11.34	10.59	8.94	7.54	7.05	4.65	4.89	4.8
Rotation (angle 110°)	12.48	11.34	10.64	8.43	7.29	6.29	5.75	5.98	5.83
Rotation (angle -50°)	12.67	11.29	10.64	8.24	7.34	7.2	6.26	6.98	6.56
Histogram Equalization	11.24	10.49	10.67	7.24	6.19	7.24	6.01	6.56	6.15
JPEG Compression (Q=20)	11.37	10.34	11.36	7.25	6.29	7.26	5.96	5.65	5.61
JPEG Compression (Q=40)	12.76	11.64	10.68	8.64	7.29	7.29	6.31	6.58	6.4
JPEG Compression (Q=60)	11.46	10.46	11.29	7.36	6.34	7.34	5.36	5.23	5.3
JPEG Compression (Q=80)	12.67	11.57	11.34	8.34	7.59	7.35	6.78	6.34	6.56
JPEG Compression (Q=100)	12.64	11.46	10.23	8.82	7.54	6.35	5.69	5.68	5.02
Median Filtering (3 X 3)	11.94	10.67	11.34	7.2	6.35	7.49	4.65	4.06	4.55
Median Filtering (5 X 5)	12.67	11.67	12.37	7.24	6.98	7.54	6.03	6.37	6.12
Weiner Filtering (3X3)	11.43	10.46	11.46	7.34	6.45	7.56	6.23	6.64	6.44
Weiner Filtering (5X5)	12.94	11.37	11.49	8.64	7.15	7.59	5.03	5.69	5.33
Gaussian Filtering (3X3)	12.93	10.67	11.49	7.15	6.68	8.15	5.45	5.89	5.55
Gaussian Filtering (5X5)	11.8	10.37	11.57	7.95	6.57	7.1	4.69	4.02	4.5
Scaling (zoomout=0.5, zoomin=2)	12.37	11.64	11.57	8.64	7.49	8.24	5.36	5.69	5.45
Scaling (zoomout=0.25, zoomin=4)	11.6	10.68	10.57	7.03	6.29	8.43	5.62	5.57	5.6
Scaling (zoomout=2, zoomin=6)	11.43	10.48	11.64	7.9	6.58	6.89	5.98	5.46	5.54
Crop 10	11.94	10.34	11.64	8.15	7.26	8.56	5.15	5.1	5.1
Crop 20	12.34	11.67	11.67	8.64	7.05	8.69	6.69	6.15	6.22
Crop 30	11.46	10.34	11.67	7.59	6.34	8.94	6.58	6.28	6.45

5.

CONCLUSION

In this research work, an innovative and blind image watermarking algorithm grounded on Fuzzy Inference System (FIS) and Human Visual System (HVS) is proposed. The results are compared with the existing method and the obtained outcomes indicates that the projected algorithm provides much more imperceptibility i.e. PSNR and robustness i.e. NCC to various image processing attacks such as Row-Column Copying, Row Column Blanking, JPEG Compression Attack, Image Contrast, Image Transformation etc., and is also more secured. In this paper, the work concerns Reversible Watermarking scheme in document images based on the two-stage FIS. The comparison experiments show that the two-stage FIS model is more suitable for the document image watermarking technology. The proposed algorithm not only has a good visual effect of the Reversible watermark and non-obstructiveness but also resists the binarization watermark removal attack. It is an effective way to achieve copyright protection of the document images.

REFERENCES

- [1] Alattar, Adnan M. (2004). "Reversible watermark using the difference expansion of a generalized integer transform". IEEE Transactions on Image Processing, Vol. 13, No. 8, pp. 1147-1156.
- [2] Shuang Yi, Yicong Zhou and Zhongyun Hua,"Reversible Data Hiding in Encrypted Images using Adaptive Block-Level PredictionError Expansion" , Journal of Signal Processing: Image Communication, pp. 1-26, 2018.
- [3] Yan Qi & Liping Liu, "Reversible Watermarking Algorithm based on Prediction Error Expansion for Color Image", Proceedings of International Conference on Image Processing, pp. 102-106, 2017.
- [4] Chan C.K, Cheng L.M. "Hiding data in images by simple LSB substitution", Pattern Recognition2004, pp 469-474.
- [5] Mathkour Hassan, Ghazy M.R., Abdulaziz Al Muharib, Ibrahim Kiady "A Novel Approach for Hiding Messages in Images", International Conference on Signal Acquisition and Processing, 2009, pp -89 – 93.
- [6] J. Feng, I. Lin, C. Tsai, Y. Chu, "Reversible watermarking: current status and key issues", Int. Journal, Vol. 2, No. 3, pp. 161– 170, 2006.
- [7] Qing Liu & Jun Ying, "Gray scale Image Digital Watermarking Technology Based on Wavelet Analysis", IEEE Symposium on Electrical & Electronics Engineering, pp. 618-621, 2012.
- [8] Khushboo Pawar, Bhawana Pillai, Dr. Sadhna K Mishra, "Conditional Local Prediction Based Image Watermarking", International Journal of Engineering Technology and Applied Science, Vol. 2 , No.3, March-2016.
- [9] Y. Hu and B. Jeon, "Reversible visible watermarking and lossless recovery of original images," IEEE Transactions on Circuits and Systems for Video Technology, vol. 12, no. 12, p. 1161, 2002.
- [10] T. Y. Liu and W. H. Tsai, "Generic lossless visible watermarking-A new approach," IEEE Transactions on Image Processing, vol. 19, no. 5, pp. 1224–1235, 2010.
- [11] C.-C. Chen, Y.-H. Tsai, and H.-C. Yeh, "Difference-expansion based reversible and visible image watermarking scheme," Multimedia Tools and Applications, vol. 76, no. 6, pp. 8497–8516, 2017.
- [12] N. Mohammad, X. Sun, H. Yang, J. Yin, G. Yang, and M. Jiang, "Lossless visible watermarking based on adaptive circular shift operation for BTC-compressed images," Multimedia Tools and Applications, vol. 76, no. 11, pp. 13301–13313, 2017.
- [13] W. Qi, G. Yang, T. Zhang, and Z. Guo, "Improved reversible visible image watermarking based on HVS and ROI-selection," Multimedia Tools and Applications, vol. 78, no. 7, pp. 8289–8310, 2019.
- [14] Y. Yao, W. Zhang, H. Wang, H. Zhou, and N. Yu, "Content-adaptive reversible visible watermarking in encrypted images," Signal Processing, vol. 164, pp. 386–401, 2019.
- [15] R. R. Selvaraju, M. Cogswell, A. Das et al., "Grad-CAM: visual explanations from deep netw

- rks via gradient-based localization,” *International Journal of Computer Vision*, vol. 128, no. 2, pp. 336–359, 2020.
- [16] J. Wu, L. Li, W. Dong, G. Shi, W. Lin, and C.-C. J. Kuo, “Enhanced Just noticeable difference model for images with pattern complexity,” *IEEE Transactions on Image Processing*, vol. 26, no. 6, pp. 2682–2693, 2017.
- [17] S. P. Mohanty, K. R. Ramakrishnan, and M. S. Kankanhalli, “A DCT domain visible watermarking technique for images,” in *Proceedings of the 2000 IEEE International Conference on Multimedia and Expo. ICME2000. Proceedings. Latest Advances in the Fast Changing World of Multimedia (Cat. No.00TH8532)*, New York, NY, USA, July 2000.
- [18] M. S. Kankanhalli, Rajmohan, and K. R. Ramakrishnan, “Adaptive visible watermarking of images,” in *Proceedings of the IEEE International Conference on Multimedia Computing and Systems*, Ottawa, Ontario, Canada, June, 1999.
- [19] Perfilieva, I. “Fuzzy transforms: theory and applications”. *Fuzzy Set Syst.* 157(8), 993–1023 (2006)
- [20] Liu, L., Chen, S., Chen, X., Wang, T., Zhang, L.” Fuzzy weighted sparse reconstruction error-steered semi-supervised learning for face recognition”. *Vis. Comput.* (2019).
- [21] Khosravian, A., Rahmimanesh, M., Keshavarzi, P., Mozaffari, S.” Fuzzy local intensity clustering (flic) model for automatic medical image segmentation”. *Vis. Comput.* (2020). <https://doi.org/10.1007/s00371-020-01861-1>
- [22] Kapoor, A., Biswas, K.K., Hanmandlu, M.” An evolutionary learning based fuzzy theoretic approach for salient object detection”. *Vis. Comput.* (2016). <https://doi.org/10.1007/s00371-016-1216-1>
- [23] Aliev, R., Tserkovny, A. “Systemic approach to fuzzy logic formalization for approximate reasoning” *Inf. Sci.* 181(6), 1045–1059 (2011)
- [24] Motwani, M.C., Harris Jr., F.C.H.”Fuzzy perceptual watermarking for ownership verification” *International Conference on Image Processing*, pp. 321–325 (2009)
- [25] Sameh-Oueslati, A.C.A., Solaiman, B. ”A fuzzy watermarking approach based on the human visual system” *Int. J. Image Process.* 3, 218–231 (2010)
- [26] Sakr, N., Zhao, J., Groza, V. “A dynamic fuzzy logic approach to adaptive HVS-based watermarking” *IEEE International Workshop on Haptic Audio Visual Environments Their Applications*, pp. 121–126 (2005)
- [27] Mortezaei, R., Moghaddam, M.E. “A new lossless watermarking scheme based on fuzzy integral and dct domain” *International Conference on Electronics and Information Engineering*, pp. 527–531 (2010)
- [28] Jagadeesh, B., Kumar, P.R., Reddy, P.C.” Robust digital image watermarking based on fuzzy inference system and back propagation neural networks using dct” *Soft. Comput.* 20(9), 3679–3686 (2016)
- [29] Salah, E., Amine, K., Redouane, K., Fares, K. “A Fourier transform based audio watermarking algorithm” *Appl. Acoust.* 172, 107652 (2021). <https://doi.org/10.1016/j.apacoust.2020.107652>
- [30] Balasamy, K., Suganyadevi, S.”A Fuzzy based ROI selection for encryption and watermarking in medical image using DWT and SVD”. *Multimedia Tools Appl.* (2020). <https://doi.org/10.1007/s11042-020-09981-5>
- [31] L. Sui and B. Gao, “Color image encryption based on gyration transform and Arnold transform,” *Optics and Laser Technology*, vol. 48, pp. 530–538, 2013.
- [32] Y.-L. Chen, H.-T. Yau, and G.-J. Yang, “A maximum entropy-based chaotic time-variant fragile: watermarking scheme for image tampering detection,” *Entropy*, vol. 15, no. 8, pp. 3170–3185, 2013.
- [33] C.-T. Hsu and J.-L. Wu, “Hidden digital watermarks in images,” *IEEE Trans. Image Process.*, vol. 8, no. 1, pp. 58–68, Jan. 1999.

[34][

19] Y. K. Lin, “A data hiding scheme based upon DCT coefficient modification,” *Comput. Standards Int.*, vol. 36, no. 56, pp. 855–862, 2014.

[35] Agarwal, Charu & Mishra, Anurag & Sharma, Arpita, “A novel gray-scale image watermarking using hybrid Fuzzy-BPN architecture”, *Egyptian Informatics Journal*. 6,2015.